Ultra-low Brillouin scattering in antiresonant hollow-core fibers

Cite as: APL Photonics 5, 096109 (2020); https://doi.org/10.1063/5.0017796 Submitted: 09 June 2020 . Accepted: 06 August 2020 . Published Online: 18 September 2020

Arjun Iyer 🗓, Wendao Xu, J. Enrique Antonio-Lopez, Rodrigo Amezcua Correa, and William H. Renninger









ARTICLES YOU MAY BE INTERESTED IN

Deep learning of ultrafast pulses with a multimode fiber APL Photonics 5, 096106 (2020); https://doi.org/10.1063/5.0007037

High-efficiency lithium niobate modulator for K band operation APL Photonics 5, 091302 (2020); https://doi.org/10.1063/5.0020040

Dynamic detection of acoustic wave generated by polarization maintaining Brillouin random fiber laser

APL Photonics 5, 096101 (2020); https://doi.org/10.1063/5.0015658





AMERICAN

Ultra-low Brillouin scattering in anti-resonant hollow-core fibers

Cite as: APL Photon. 5, 096109 (2020); doi: 10.1063/5.0017796 Submitted: 9 June 2020 • Accepted: 6 August 2020 •







Published Online: 18 September 2020

Arjun Iyer, 1a) D Wendao Xu, J. Enrique Antonio-Lopez, Rodrigo Amezcua Correa, and William H. Renninger

AFFILIATIONS

- ¹Institute of Optics, University of Rochester, Rochester, New York 14627, USA
- ²CREOL, The College of Optics and Photonics, University of Central Florida, Orlando, Florida 32816, USA

ABSTRACT

Sensitive optical experiments in fiber, including for applications in communications and quantum information, are limited by the noise generated when light scatters from thermally excited guided-acoustic phonons. Novel fibers, such as microstructured fibers, offer control over both optical and acoustic waveguide properties, which can be designed to mitigate optomechanical noise. Here, we investigate the optomechanical properties of microstructured anti-resonant hollow-core fibers and demonstrate their promise as a low-noise fiber platform. By developing an ultra-sensitive spectroscopy technique, a seven capillary anti-resonant hollow-core fiber is found to exhibit record low optomechanical coupling ($<10^{-4} \text{ W}^{-1} \text{ m}^{-1}$), in agreement with comprehensive numerical calculations. The largest scattering occurs from a guided acoustic mode in the air confined in the core of the fiber. Acoustic resonances in the silica, due to minimal overlap with the optical mode in the core, scatter a hundred times less, resulting in negligible depolarization noise. The largest optomechanical interactions in anti-resonant hollow-core fibers are found to be at least three (five if evacuated) orders of magnitude weaker than those in conventional single-mode fibers, which makes this class of fibers a promising platform for low noise applications, including quantum information processing and optical communication.

© 2020 Author(s). All article content, except where otherwise noted, is licensed under a Creative Commons Attribution (CC BY) license (http://creativecommons.org/licenses/by/4.0/). https://doi.org/10.1063/5.0017796

I. INTRODUCTION

Light scatters from guided acoustic waves through a nonlinear optomechanical interaction referred to as guided acoustic wave Brillouin scattering. Thermally excited guided acoustic phonons can scatter incident light to new up-shifted (anti-Stokes) and downshifted (Stokes) optical frequencies [Fig. 1(a)]. The scattered optical waves propagate in the same direction as the incident light, in contrast to traditional Brillouin scattering in which the incident and scattered waves counter-propagate. 1-4 These so-called forward Brillouin interactions are valuable for applications, including highperformance sensors, 5-7 on-chip Brillouin lasers, 8-10 RF filters, 1 isolators, 14,15 and amplifiers. 16,17 However, forward optomechanical interactions can also produce an unwanted source of noise in optical systems and can lead to quantum decoherence in quantum information systems. Forward Brillouin scattering in fibers has been shown to exceed the shot-noise limit 18-24 and presents fundamental limitations to quantum operations such as squeezing, 21-23,25 entanglement generation and distribution, ²⁶ quantum state communication, ²⁷ and quantum key distribution.²⁸ This optomechanical noise degrades the signal quality in conventional optical communication systems as well.²⁹ Techniques for mitigating forward Brillouin scattering in fibers involve complex solutions such as cryogenic cooling²³ or quantum error-correcting algorithms.²⁷ An improved understanding of forward Brillouin interactions is needed for engineering a new practical approach for mitigating optomechanical noise in fibers.

Photonic crystal fibers (PCFs) enable a wide range of possibilities for customizing the properties of an optical waveguide. 30,31 The optomechanical properties and prospects of these fibers have recently attracted interest as well. For example, PCFs have been explored for significantly enhancing the forward Brillouin interaction. Strong confinement is possible for both the optical and acoustic waves within the solid core of a PCF, resulting in almost two-orders of magnitude more optomechanical coupling than in standard fibers. PCFs also open up new pathways toward reducing optomechanical interactions and noise. Hollow-core PCFs, for example, which guide light in a hollow-core, avoid the dominant

a) Author to whom correspondence should be addressed: aiyer2@ur.rochester.edu

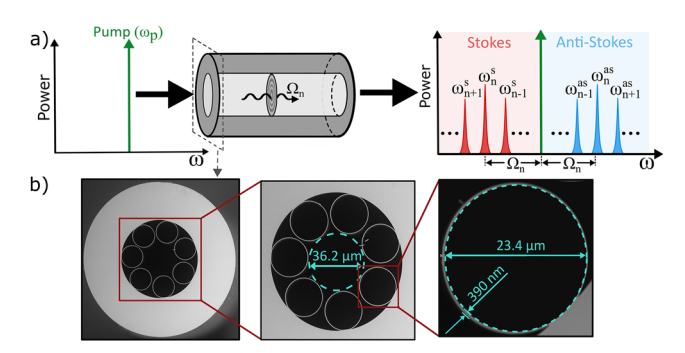


FIG. 1. Forward Brillouin scattering in fiber. (a) The salient frequencies participating in the interaction. A single frequency pump coupled into an optical fiber scatters from thermally excited guided acoustic phonons with frequency Ω_n into Stokes (ω_n^s) and anti-Stokes (ω_n^{as}) sidebands with linewidths (Γ_n) determined by the acoustic dissipation in the medium. (b) SEM cross section of the ARHCF under investigation.

interaction with acoustic waves in the silica core. However, the guided light can interact with acoustic waves supported by the microstructured silica cladding, which introduces considerable undesirable scattering and depolarization noise. ^{18,19,33,34} The residual air, or other gas, in the core supports guided acoustic waves as well, providing an additional source of noise. ³⁴ While PCFs can offer reduced overall scattering in comparison with conventional fiber, further reduction in noise will require an alternative cross-sectional design, which is complicated theoretically and experimentally by the geometrically intricate silica microstructure. ³³

Anti-Resonant Hollow-Core Fibers (ARHCFs) are an emerging class of hollow-core fibers that enable new opportunities for optomechanical interactions. ARHCFs guide light through an inhibitedcoupling design that strongly reduces the coupling of light in the core to the continuum of cladding modes.³⁵ have gained attention recently owing to their ultra-low loss across broad bandwidths, 40-43 strong optical confinements, 44 high damage thresholds, 45 and relatively simple fabrication requirements. While little is known to date about the optomechanical properties of ARHCFs, the unique geometrical structure of ARHCFs featuring sparse, thin segments of silica may enable new opportunities for optomechanical interactions. In addition, the tight confinement of the optical mode and lack of material in and around the core suggest that these fibers could be an attractive alternative for suppressing optomechanical noise for sensitive applications. However, characterizing such weak optomechanical effects will require measurement sensitivities significantly beyond those demonstrated in previous investigations of forward Brillouin scattering.3

In this manuscript, we detail the comprehensive characterization of optomechanical interactions in an air-filled seven-capillary ARHCF [Fig. 1(b)] theoretically and experimentally for the first time. Measurements are made with a modified spectroscopy technique capable of achieving sensitivities improved by two orders of magnitude over previous results. Experimental results are explained through a simple physical model, and approaches toward improved optomechanical gain sensitivities are identified.

II. THEORY

Optical fields in a waveguide stimulate resonant acoustic modes through electrostrictive and radiation pressure forces. Once generated, guided acoustic modes modulate the refractive index, which scatters incident light into Stokes and anti-Stokes sidebands [Fig. 1(a)], inducing a phase modulation on the incident optical field.^{2,33} The relative strength of the scattered light (the modulation depth of the induced phase modulation), or optical noise, can be quantified with an optomechanical (Brillouin) interaction gain. Brillouin gain, determined by energy conservation, is calculated using the specific spatial distribution of the optical and acoustic modes in the fiber under consideration. These modes are calculated numerically for ARHCF using finite element simulations. The incident and scattered optical fields are designed to be guided by the fundamental propagation mode of the fiber. Simulations reveal an axially symmetric, linearly polarized, HE11-like optical mode with a mode-field diameter of 28.7 μ m [Fig. 2(a)]. The electrostrictive force from light guided by this mode is radial with an annular distribution [Fig. 2(b)]. The acoustic modes can be classified as being either supported by the air confined in the core or supported by the surrounding silica capillaries and cladding. The silica resonances are densely arranged in frequency with a variety of displacement distributions, similar to those in hollow-core PCFs. 18,5 The acoustic modes supported in air are found to have radial displacement with Bessel-like spatial profiles [Figs. 2(c) and 2(d)]. These modes resemble the Bessel-shaped modes supported by air in a rigid hollow cylinder, but with noticeable perturbations stemming from the thin silica capillaries. The frequencies of these resonances can be predicted using a simple model that combines the Bessel modes from a cylinder with the radius of the core with those from a cylinder with the radius that extends to the beginning of the solid silica cladding (see the supplementary material). This simple model is expected to be relevant to fibers beyond this specific structure, given the structural similarity of a wide range of ARHCFs.4

The Brillouin coupling strength is proportional to the spatially integrated vectoral overlap between the optical forcing and the

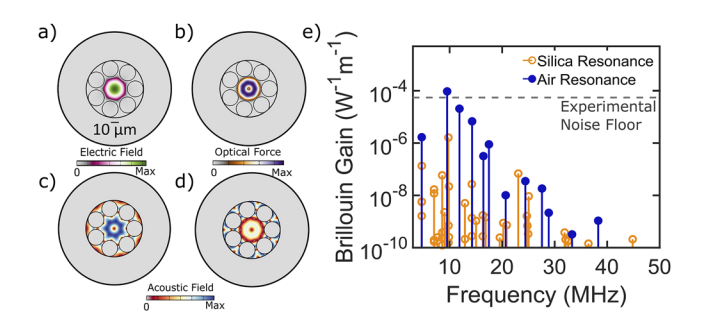


FIG. 2. Numerical calculations of the forward Brillouin response of the ARHCF. (a) The electric field distribution of the fundamental optical mode of the ARHCF. (b) The electrostrictive force distribution produced by light from the fundamental optical mode. The absolute value of transverse radial displacement for the air-supported acoustic modes with the (c) first and (d) second highest optomechanical coupling. (e) Calculated Brillouin gain for acoustic modes supported by the air-filled core (blue) and acoustic modes supported by the surrounding silica (orange) for the case where the incident and scattered fields are co-polarized (relative to the probe).

acoustic displacement distributions. 47,48 Electrostriction within the material is found to be the dominant contribution to the optical forcing, larger than surface forces from electrostriction and radiation pressure^{3,48,49} (see the supplementary material). The forcing distribution within the material [Fig. 2(b)] closely overlaps with acoustic modes supported by the air confined in the core of the fiber [Figs. 2(c) and 2(d)], leading to the largest gain for this family of modes. Brillouin gain is calculated for all the simulated guided acoustic modes and plotted as a function of frequency [Fig. 2(e)]. Results are shown for the case where the incident field and the scattered fields are co-polarized relative to the probe. Coupling is significantly reduced if the fields are counter-polarized (see the supplementary material). A single resonance is anticipated to produce a signal that rises above the experimental noise floor of the spectroscopy described below. This resonance, from the family of Bessellike modes supported by air [Fig. 2(c)], has a resonant frequency of 9.4 MHz and a Brillouin gain of $9 \times 10^{-5} \text{ W}^{-1} \text{ m}^{-1}$. The reduced coupling compared to previous fibers can be understood because (1) the optical and acoustic mode sizes are larger and (2) the optomechanical overlap is reduced because while the light is confined to the core, the acoustic mode extends to the inner cladding. The other acoustic modes supported by air [indicated by blue in Fig. 2(e)] have a weaker overlap with the optical forcing distribution, which corresponds to reduced coupling. The acoustic resonances supported by silica [indicated by orange in Fig. 2(e)] have much lower overlap with the optical forcing in the core and consequently have coupling strengths that are at least two orders of magnitude lower than the acoustic resonances supported by air.

III. EXPERIMENTAL RESULTS

Sensitive forward Brillouin spectroscopy is developed experimentally based on a two-color technique^{33,34} (see the supplementary material). An optical drive is first generated by modulating a narrowlinewidth laser with a carrier-suppressed intensity modulator. The interference between the resultant two optical frequencies resonantly drives the acoustic modes when the modulation frequency matches the frequency of the acoustic resonance. A second, probe laser, separated by several nanometers in wavelength from the drive laser, scatters from the driven acoustic resonances to generate Stokes and anti-Stokes sidebands. In contrast to backward Brillouin scattering, optical fields widely separated in wavelength can interact via the same acoustic mode because weak group velocity dispersion leads to an acoustic mode wavevector that changes negligibly as a function of the optical wavelength.³³ The scattered sidebands are distinguished through a heterodyne detection process through which the scattered fields are mixed with an optical tone that is frequency upshifted from the probe laser using an acousto-optic modulator. The swept spectral response of the measurement is a coherent sum of the resonant Brillouin interactions of interest and a frequency independent background resulting from Kerr four-wave mixing and interference effects, leading to well-known Fano-like resonance profiles.³³ The experimentally observed Brillouin resonances are numerically fit to obtain the center frequency, linewidth, and on-resonance Stokes (or anti-Stokes) sideband power. The optomechanical coupling strength (G) is determined using the on-resonance Stokes power (P_s) , acoustic drive powers (P_{p1}, P_{p2}) , probe power (P_{pr}) , and the length of the

fiber (L) under test using the relation $P_s = (\frac{1}{4})G^2L^2P_{p1}P_{p2}P_{pr}$. The experimental sensitivity is found to be primarily limited by the nonresonant background arising from mismatched optical paths of the probe and reference arms. Path mismatch is minimized by monitoring the noise spectrum of the heterodyne interference signal in the absence of the acoustic drive. This noise spectrum arising from the finite optical linewidths of the laser sources is used as a signature for path length mismatch minimization.⁵⁰ Optimization through this procedure enables fW sensitivity and the ability to resolve Brillouin gain coefficients at the level of $2 \times 10^{-5} \text{ W}^{-1} \text{ m}^{-1}$. At this low signal level, conventional numerical fitting procedures are insufficient to extract optomechanical gain coefficients, and additional considerations become important, such as non-unique optomechanical gain coefficients (see the supplementary material for further details). Previous measurements, in hollow-core PCFs, reported a gain sensitivity at the level of $1 \times 10^{-4} \text{ W}^{-1} \text{ m}^{-1}$ but with acoustic drive powers roughly a factor 3 larger than acoustic drive powers employed in our work.³³ Altogether, the experimental technique demonstrated here features Stokes power sensitivities improved by ~225 times or, equivalently, gain sensitivities improved ~15 times. Previous techniques lack the signal-to-noise ratio needed to characterize guided optomechanical processes inside anti-resonant hollow-core fibers. Further suppression of the non-resonant background could enable sensitivities that are limited only by the Kerr nonlinearity of the medium.

The optomechanical spectral response of a 1-m long air-filled seven-capillary ARHCF is characterized to frequencies up to 50 MHz. A single resonance is observed above the noise floor for measurements where the scattered signal is co-polarized relative to the input probe [Fig. 3(a)]. This resonance is found at 9.4 MHz, with a linewidth of 1.6 MHz and an optomechanical coupling strength of $8.6 \times 10^{-5} \ \text{W}^{-1} \ \text{m}^{-1}$. The resonance frequency and coupling strength agree well with theoretical predictions, and the linewidth is consistent with the acoustic loss known for 10-MHz acoustic waves in air. No additional resonances are observed over the noise floor regardless of whether the scattered signal is co-[Fig. 3(a)] or counter-polarized [Fig. 3(b)] relative to the input probe, in agreement with theoretical predictions. In stark contrast

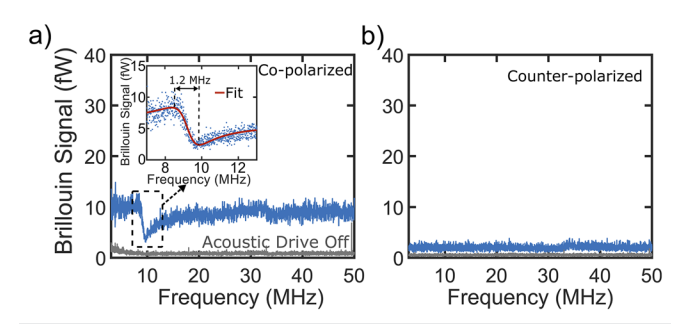


FIG. 3. Measured forward Brillouin response of the ARHCF. (a) Co-polarized (relative to the probe) optomechanical response as a function of drive frequency (blue). The distinct resonance at 9.4 MHz is the inset with an analytical fit in red. This signature is absent when the acoustic drive is off (gray). (b) No optomechanical signatures are observed from the orthogonally polarized scattered light (relative to the probe) with (blue) or without (gray) the acoustic drive.

to previous measurements of hollow-core PCFs, no response corresponding to acoustic resonances supported by the silica is observed. The weak feature near 33 MHz in Figs. 3(a) and 3(b) was verified as a radiofrequency artifact originating from the experimental setup.

IV. DISCUSSION AND CONCLUSION

In this work, we report on nonlinearities inside a 7-capillary ARHCF from an acoustic resonance supported by the air confined to the fiber core. The optomechanical coupling is reduced from previous hollow-core fibers because the effective mode sizes of the optical and acoustic modes are larger and because the optomechanical overlap is reduced owing to their unequal sizes. If the gas in the hollow fiber were evacuated, the optomechanical response and corresponding noise from this fiber would be reduced to the level of scattering from the silica alone, which is two orders of magnitude weaker. The optomechanical response is measured with a two-color pumpprobe scheme combined with a heterodyne readout. The sensitivity of this technique is currently limited by the common mode noise arising from residual optical path length mismatch between the signal and reference paths used for heterodyne readout. By reducing this mismatch from the cm to mm scale, we expect the sensitivity to improve further. This work presents some of the most sensitive measurements of optomechanical nonlinearities to date. While recipes have been suggested previously for obtaining lower optomechanical couplings, they have not yet been validated experimentally. The ability to measure optomechanical interactions with previously unattained sensitivities could enable measurements of qualitatively new phenomena in other optomechanical systems as well.

This study also suggests alternative uses for ARHCF. For example, this fiber may be valuable in the opposite limit of very strong optomechanical coupling. A larger overlap between the optical mode and the acoustic mode in the gas-filled core can be engineered by adjusting the fiber parameters appropriately. In addition, the coupling can be increased significantly by either increasing the gas pressure or operating near an atomic resonance. This fiber would benefit from large gas coupling without additional unwanted interactions with the surrounding silica microstructure. A high-gain ARHCF system could, therefore, enable a powerful new technique for sensing, lasers, and signal processing.

In this report, we demonstrate record-low optomechanical nonlinearities in anti-resonant hollow-core fibers. We measure this ultra-low coupling through an improved phonon mediated four-wave mixing experimental technique, allowing us to achieve two orders of magnitude improved optomechanical sensitivities than in previous studies. The maximum optomechanical coupling in these fibers is found to be a thousand times lower than that from single-mode fibers, an order of magnitude lower than that from alternative hollow-core fibers, and with negligible scattering from the surrounding silica microstructure. This ultra-low optomechanical noise and negligible depolarization noise makes this class of fibers ideal for low-noise applications, including quantum information processing and optical communication.

SUPPLEMENTARY MATERIAL

See the supplementary material for an approximate model of the fiber acoustic resonances, further details regarding the experimental setup and analysis, and additional experimental and numerical results.

ACKNOWLEDGMENTS

This research was funded by the National Science Foundation (NSF) (Grant No. 1943658), the Army Research Office (Grant No. W911NF-17-1-0501), and the University of Rochester.

DATA AVAILABILITY

The data that support the findings of this study are available from the corresponding author upon reasonable request.

REFERENCES

- ¹ R. M. Shelby, M. D. Levenson, and P. W. Bayer, "Guided acoustic-wave Brillouin scattering," Phys. Rev. B **31**, 5244–5252 (1985).
- ²M. S. Kang, A. Nazarkin, A. Brenn, and P. S. J. Russell, "Tightly trapped acoustic phonons in photonic crystal fibres as highly nonlinear artificial Raman oscillators," Nat. Phys. 5, 276–280 (2009).
- ³P. T. Rakich, P. Davids, and Z. Wang, "Tailoring optical forces in waveguides through radiation pressure and electrostrictive forces," Opt. Express 18, 14439 (2010).
- ⁴G. Mélin, H. Maillotte, J.-C. Beugnot, T. Sylvestre, and V. Laude, "Guided acoustic wave Brillouin scattering in photonic crystal fibers," Opt. Lett. **32**(1), 17–19 (2007).
- ⁵Y. Antman, A. Clain, Y. London, and A. Zadok, "Optomechanical sensing of liquids outside standard fibers using forward stimulated Brillouin scattering," Optica 3, 510 (2016).
- ⁶D. M. Chow, Z. Yang, M. A. Soto, and L. Thévenaz, "Distributed forward Brillouin sensor based on local light phase recovery," Nat. Commun. **9**, 2990 (2018).
- ⁷D. M. Chow and L. Thévenaz, "Forward Brillouin scattering acoustic impedance sensor using thin polyimide-coated fiber," Opt. Lett. **43**, 5467 (2018).
- ⁸N. T. Otterstrom, R. O. Behunin, E. A. Kittlaus, Z. Wang, and P. T. Rakich, "A silicon Brillouin laser," Science **360**, 1113–1116 (2018).
- ⁹S. Gundavarapu, G. M. Brodnik, M. Puckett, T. Huffman, D. Bose, R. Behunin, J. Wu, T. Qiu, C. Pinho, N. Chauhan, J. Nohava, P. T. Rakich, K. D. Nelson, M. Salit, and D. J. Blumenthal, "Sub-hertz fundamental linewidth photonic integrated Brillouin laser," Nat. Photonics 13, 60–67 (2019).
- ¹⁰S. Han, D. G. Kim, J. Hwang, I. Hwan Do, D. Jeong, Y. H. Lee, D. Y. Choi, and H. Lee, "On-chip stimulated Brillouin lasers based on chalcogenide glass resonators with 10 million Q-factor," in *Proceedings of the 2019 Conference on Lasers and Electro-Optics, CLEO 2019* (Optical Society of America, 2019), pp. 2–3.
- ¹¹E. A. Kittlaus, P. Kharel, N. T. Otterstrom, Z. Wang, and P. T. Rakich, "RF-photonic filters via on-chip photonic-phononic emit-receive operations," J. Lightwave Technol. 36, 2803–2809 (2018).
- ¹²A. Choudhary, Y. Liu, B. Morrison, K. Vu, D. Y. Choi, P. Ma, S. Madden, D. Marpaung, and B. J. Eggleton, "High-resolution, on-chip RF photonic signal processor using Brillouin gain shaping and RF interference," Sci. Rep. 7, 5932 (2017)
- ¹³Y. Stern, K. Zhong, T. Schneider, R. Zhang, Y. Ben-Ezra, M. Tur, and A. Zadok, "Tunable sharp and highly selective microwave-photonic band-pass filters based on stimulated Brillouin scattering," Photonics Res. 2, B18 (2014).
- ¹⁴J. Kim, M. C. Kuzyk, K. Han, H. Wang, and G. Bahl, "Non-reciprocal Brillouin scattering induced transparency," Nat. Phys. 11, 275–280 (2015).
- ¹⁵C. H. Dong, Z. Shen, C. L. Zou, Y. L. Zhang, W. Fu, and G. C. Guo, "Brillouin-scattering-induced transparency and non-reciprocal light storage," Nat. Commun. 6, 6193 (2015).
- ¹⁶E. A. Kittlaus, H. Shin, and P. T. Rakich, "Large Brillouin amplification in silicon," Nat. Photonics 10, 463–467 (2016).

- ¹⁷T. Baehr-Jones, R. Shi, and D. J. Blumenthal, "Nonlinear optics: Enhanced Brillouin amplification in Si," Nat. Photonics 10, 432–434 (2016).
- ¹⁸W. E. N. Zhong, B. Stiller, D. Elser, B. Heim, C. Marquardt, and G. Leuchs, "Depolarized guided acoustic wave Brillouin scattering in hollow-core photonic crystal fibers," Opt. Express 23, 27707 (2015).
- ¹⁹D. Elser, U. L. Andersen, A. Korn, O. Glöckl, S. Lorenz, C. Marquardt, and G. Leuchs, "Reduction of guided acoustic wave Brillouin scattering in photonic crystal fibers," Phys. Rev. Lett. 97, 133901 (2006).
- ²⁰D. Elser, C. Wittmann, U. L. Andersen, O. Glöckl, S. Lorenz, C. Marquardt, and G. Leuchs, "Guided acoustic wave Brillouin scattering in photonic crystal fibers," J. Phys.: Conf. Ser. **92**, 012108 (2007).
- ²¹M. Shirasaki and H. A. Haus, "Reduction of guided-acoustic-wave Brillouin scattering noise in a squeezer," Opt. Lett. 17, 1225 (1992).
- ²² K. Bergman and H. A. Haus, "Squeezing in fibers with optical pulses," Opt. Lett. 16, 663 (1991).
- ²³ R. M. Shelby, M. D. Levenson, S. H. Perlmutter, R. G. Devoe, and D. F. Walls, "Broad-band parametric deamplification of quantum noise in an optical fiber," Phys. Rev. Lett. 57, 691–694 (1986).
- ²⁴Y. Sakai, R. J. Hawkins, and S. R. Friberg, "Soliton-collision interferometer for the quantum nondemolition measurement of photon number: Numerical results," Opt. Lett. **15**, 239 (1990).
- ²⁵K. Bergman, C. R. Doerr, H. A. Haus, and M. Shirasaki, "Sub-shot-noise measurement with fiber-squeezed optical pulses," Opt. Lett. 18, 643 (1993).
- ²⁶J. Feng, Z. Wan, Y. Li, and K. Zhang, "Distribution of continuous variable quantum entanglement at a telecommunication wavelength over 20 km of optical fiber," Opt. Lett. 42, 3399 (2017).
- ²⁷ M. Lassen, A. Berni, L. S. Madsen, R. Filip, and U. L. Andersen, "Gaussian error correction of quantum states in a correlated noisy channel," Phys. Rev. Lett. 111, 180502 (2013).
- ²⁸Y. Li, N. Wang, X. Wang, and Z. Bai, "Influence of guided acoustic wave Brillouin scattering on excess noise in fiber-based continuous variable quantum key distribution," J. Opt. Soc. Am. B **31**, 2379 (2014).
- ²⁹ M. Nakazawa, M. Yoshida, M. Terayama, S. Okamoto, K. Kasai, and T. Hirooka, "Observation of guided acoustic-wave Brillouin scattering noise and its compensation in digital coherent optical fiber transmission," Opt. Express 26, 9165 (2018).
- ³⁰J. C. Knight, "Photonic band gap guidance in optical fibers," Science 282, 1476–1478 (1998).
- ³¹J. M. Dudley, G. Genty, and S. Coen, "Supercontinuum generation in photonic crystal fiber," Rev. Mod. Phys. **78**, 1135–1184 (2006).
- ³²P. Dainese, A. Khelif, G. S. Wiederhecker, H. L. Fragnito, N. Joly, P. S. Russell, and V. Laude, "Raman-like light scattering from acoustic phonons in photonic crystal fiber," Opt. Express 14(9), 4141–4150 (2006).
- ³³W. H. Renninger, H. Shin, R. O. Behunin, P. Kharel, E. A. Kittlaus, and P. T. Rakich, "Forward Brillouin scattering in hollow-core photonic bandgap fibers," New J. Phys. 18, 025008 (2016).
- ³⁴W. H. Renninger, R. O. Behunin, and P. T. Rakich, "Guided-wave Brillouin scattering in air," Optica 3, 1316–1319 (2016).
- ³⁵B. Debord, A. Amsanpally, M. Chafer, A. Baz, M. Maurel, J. M. Blondy, E. Hugonnot, F. Scol, L. Vincetti, F. Gérôme, and F. Benabid, "Ultralow transmission loss in inhibited-coupling guiding hollow fibers," Optica 4, 209 (2017).

- ³⁶B. Debord, A. Amsanpally, M. Chafer, A. Baz, L. Vincetti, J. M. Blondy, F. Gérôme, and F. Benabid, "7.7 dB/km losses in inhibited coupling hollow-core photonic crystal fibers," in 2016 Conference on Lasers and Electro-Optics, CLEO 2016 (Optical Society of America, 2016), pp. 9–10.
- ³⁷F. Couny, F. Benabid, and P. S. Light, "Large pitch Kagome-structured hollow-core photonic crystal fiber," Opt. Lett. 31, 3574–3576 (2006).
- ³⁸F. Couny, F. Benabid, P. J. Roberts, P. S. Light, and M. G. Raymer, "Generation and photonic guidance of multi-octave optical-frequency combs," Science 318, 1118–1121 (2007).
- ³⁹Y. Y. Wang, N. V. Wheeler, F. Couny, P. J. Roberts, and F. Benabid, "Low loss broadband transmission in hypocycloid-core Kagome hollow-core photonic crystal fiber," Opt. Lett. 36, 669 (2011).
- ⁴⁰J. C. Knight, "Anti-resonant hollow core fibers," in *Proceedings of the 2019 Optical Fiber Communications Conference and Exhibition, OFC 2019* (Optical Society of America, 2019), pp. 40–42.
- ⁴¹T. Bradle, J. Hayes, L. Hooper, H. Sakr, G. Jasion, M. Alonso, A. Taranta, A. Saljoghei, M. Fake, I. Davidson, Y. Chen, N. Wheeler, E. Fokoua, W. Wang, S. Reza Sandoghchi, D. Richardson, F. Poletti, and H. Christian Mulvad, "Antiresonant hollow core fibre with 0.65 dB/km attenuation across the C and L telecommunication bands," in 45th European Conference on Optical Communication (ECOC 2019) (IEEE, 2019), p. PDP3.1.
- ⁴²G. T. Jasion, T. Bradley, K. Harrington, H. Sakr, Y. Chen, E. Numkam Fokoua, I. Davidson, A. Taranta, J. Hayes, D. Richardson, and F. Poletti, "Hollow core NANF with 0.28 dB/km attenuation in the C and L bands," in *Optical Fiber Communication Conference* 2020 (The Optical Society, 2020), p. Th4B.4.
- ⁴³T. D. Bradley, J. R. Hayes, Y. Chen, G. T. Jasion, S. R. Sandoghchi, and R. Slavik,
 "Record low-loss 1.3 dB/km data transmitting antiresonant hollow core fibre," in
 European Conference on Optical Communication (ECOC) (IEEE, 2018), pp. 1–3.
 ⁴⁴S.-F. Gao, Y.-Y. Wang, W. Ding, and P. Wang, "Hollow-core negative-curvature
- fiber for UV guidance," Opt. Lett. **43**, 1347 (2018).

 ⁴⁵M. Michieletto, J. K. Lyngsø, C. Jakobsen, J. Lægsgaard, O. Bang, and T. T. Alkeskjold, "Hollow-core fibers for high power pulse delivery," Opt. Express **24**,
- 7103 (2016).

 46 F. Yu and J. Knight, "Negative curvature hollow core optical fiber," IEEE J. Sel.
- Top. Quantum Electron. 22, 1 (2015).

 47 W. Qiu, P. T. Rakich, H. Shin, H. Dong, M. Soljačić, and Z. Wang, "Stimulated Brillouin scattering in nanoscale silicon step-index waveguides: A general framework of selection rules and calculating SBS gain," Opt. Express 21, 31402
- ⁴⁸C. Wolff, M. J. Steel, B. J. Eggleton, and C. G. Poulton, "Stimulated Brillouin scattering in integrated photonic waveguides: Forces, scattering mechanisms, and coupled-mode analysis," Phys. Rev. A **92**, 013836 (2015).
- ⁴⁹C. G. Poulton, R. Pant, and B. J. Eggleton, "Acoustic confinement and stimulated Brillouin scattering in integrated optical waveguides," J. Opt. Soc. Am. B **30**, 2657 (2013).
- ⁵⁰ L. Richter, H. Mandelberg, M. Kruger, and P. McGrath, "Linewidth determination from self-heterodyne measurements with subcoherence delay times," IEEE J. Quantum Electron. 22, 2070–2074 (1986).
- L. J. Bond, C.-H. Chiang, and C. M. Fortunko, "Absorption of ultrasonic waves in air at high frequencies (10–20 MHz)," J. Acoust. Soc. Am. 92, 2006–2015 (1992).
 L. Thévenaz, F. Gyger, and F. Yang, "Large Brillouin interaction in hollow core fibers," Asia Communications and Photonics Conference (ACP) (IEEE, 2019), pp. 1–3.